Simulation Analysis of Tunnel Vision Effect in Crowd Evacuation

Akira Tsurushima[(✉)]

Intelligent Systems Laboratory, SECOM CO., LTD., Mitaka, Tokyo, Japan
`a-tsurushima@secom.co.jp`

Abstract. Excessive cognitive demands, fear, or stress narrow evacuees' functional fields of view (FFV) in disaster evacuation situations. This tunnel vision hypothesis leads to a new model of evacuee behavior deviating significantly from the previously accepted understanding, and possibly altering conventional evacuation protocol designs. In this study, we analyze the impacts of narrowed vision of evacuees on crowd evacuation efficiency through simulated evacuations. The simulated room to be evacuated included multiple exits, of which only one was correct, as well as a single visual sign designating the correct exit, and an agent found the correct exit via this sign if it was within their FFV. We designed an evacuation decision model for the simulated agents based on herd behavior, including cognitive biases frequently observed during evacuations, to which evacuees were assumed to be subject.

Keywords: Tunnel vision · Herd behavior · Evacuation decision model

1 Introduction

Mackworth (1965) introduced the concept of tunnel vision, a narrowing of the human FFV owing to excessive cognitive demand, stress, or fear [7]; numerous studies on the subject have since been conducted [1–3,6]. In tunnel vision, human cognitive resources focus on the center of the visual field, resulting in a loss object perception outside of this focus, especially in the peripheral vision. Furthermore, tunnel vision has been shown to occur during violent crimes and emergency situations, and to affect operators of complex systems and vehicle drivers; its effects are known to lead to loss of life or damage to property in some cases.

Although several conditions common in disaster evacuation situations are understood to cause tunnel vision, prior research on crowd evacuation has rarely focused on the human FFV. Most crowd evacuation studies using experiments or simulations have assumed the FFV of an agent arbitrary or implicitly, or simply considered the range at which an agent could perceive objects as their FFV. As yet, few studies have explored the human FFV based on physiological or psychological factors.

The FFV of an evacuee is crucial in crowd evacuations for two reasons. (1) The FFV of any agent bounds other agents considered in models of herd behavior among evacuees, affecting the behavior of the crowd as a whole. (2) Visual

information such as exit signs or evacuation route signs are commonly used to efficiently guide crowd evacuations, and agents are able to recognize such signs only within their FFV.

Presenting a simulation analysis of evacuation behaviors among people appearing in a video clip captured during the Great East Japan Earthquake, Tsurushima (2020) introduced the *tunnel vision hypothesis* that the human FFV during emergency evacuation situations narrows to an angle of 20° toward the heading direction, with a relatively long range [14]. While numerous studies on crowd evacuation have adopted a wide visual field, such as 120° or 360°, the tunnel vision hypothesis introduced a much narrower visual field, restricted to 20°. The significant difference in visual range and scope between the predictions of the tunnel vision hypothesis and the conventional assumptions may alter previously accepted research results on crowd evacuation. The impact of the tunnel vision hypothesis may be crucial, especially for research on emergency evacuation protocol design using visual communication for critical information.

This study analyzes the impact of tunnel vision effects on crowd evacuation using two simple simulation problems. Both problem scenarios concern an environment with two exits, one being designated by a visual sign. The objective of both problems was to maximize the number of agents reaching a correct exit designated by a visual sign, by varying the position of the sign within the simulated environment. Exit choice decisions in crowd evacuations are highly complex; aside from visual signs, herd behaviors among evacuees also affect individuals' decisions by propagating both correct and incorrect information within a crowd. Thus, directing a crowd to a correct exit can prove challenging. We investigated the impact of tunnel vision on crowd exit choice decisions by comparing simulated agents with tunnel vision and with normal (wider) vision.

2 Related Works

Several studies of psychological and cognitive factors on evacuation behavior have been conducted using virtual reality (VR) devices. Tucker et al. (2018) investigated the impact of hazard levels on evacuees' anxiety and exit route decisions using VR, and showed that evacuees tended significantly to select a major exit rather than peripheral exits under highly hazardous conditions [15]. Meng and Zhang (2014) conducted evacuation experiments simulating a hotel fire incident using VR, analyzing simulations with and without conditions of virtual fire, and found that evacuees required more time to find evacuation signs and exits in simulated fire emergency conditions [9]. New approaches using shared virtual spaces with multiple subjects have recently emerged. Mousaid et al. (2018) conducted VR evacuation experiments in settings with four exits, of which one was randomly selected as correct, in which a subset of the subjects knew the correct exit in advance. They analyzed evacuation behaviors under stressful emergency conditions and under non-stressful conditions, and showed that a higher number of collisions occurred under high-stress conditions, and a majority of participants moved as a herd in the same direction [10]. VR evacuation experiments
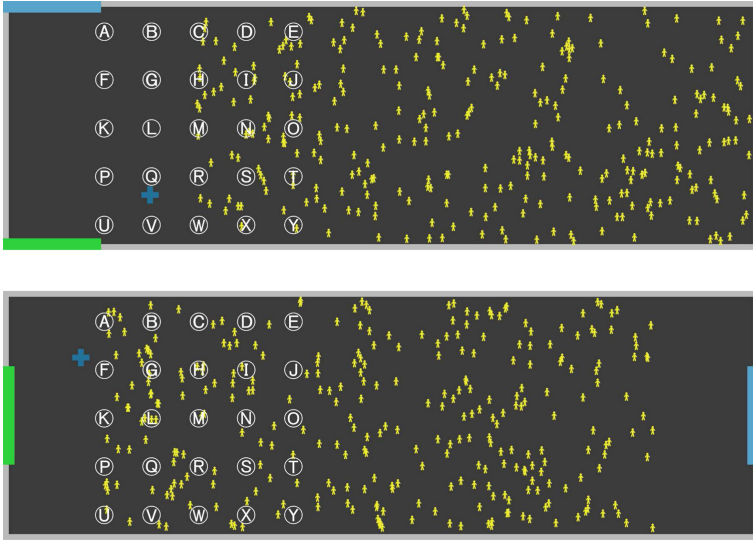
Fig. 1. Room1 (top) and Room 2 (bottom) (Color figure online)

have shown promise in investigations of cognitive factors in evacuations; however, to the best of our knowledge, as yet no prior studies have been conducted using VR concerning the visual fields of evacuees.

Li et al. (2019) introduced a visibility function and investigated the effects of several factors on evacuation efficiency, such as psychological tension, vision radius, and pedestrian density. They found that vision radius and initial density affected evacuation time, and that vision radius decreased with increasing evacuation time [5]. The authors did not restrict the angular width of the evacuees' visual fields, assuming instead that they could acquire information within 360°. Similar assumptions have been adopted in numerous studies [16–18]. Some studies have been conducted employing visual field widths other than 360°, such as 60° [8] and 90° [11]; however, their reasons for choosing these assumptions were not clearly stated.

3   Problem

Three hundred simulated agents ($a_i \in A$) were randomly distributed in a square room with XY coordinates $x \in [-65, 65]$ and $y \in [-20, 20]$, and agents were required to evacuate through either of two exits $B = \{b^+, b^-\}$. The coordinates of an exit b are denoted by (b_x, b_y). We investigated two layouts according to the location of the exits. Room 1 had two exits on the north (blue) and south (green) sides of the western edge of the room (Fig. 1 – top). Agents were initially allocated to $x_i \in [-32, 65]$ and faced west. Room 2 had two exits on the east (blue) and west (green) edges of the room (Fig. 1 – bottom). Agents were initially

Algorithm 1. Agent i's action ($X_i = 0$)

1: $M \leftarrow \{a_j \in V_i | \eta_j = moving\}$; $N \leftarrow \{a_j \in V_i | \eta_j = not\_moving\}$
2: **if** $|M| > |N|$ **then**
3:      **if** $\exists m \forall n |\{a_j \in V_i | \pi_j = \beta_m\}| \geq |\{a_k \in V_i | \pi_k = \beta_n\}|$ **then** $\pi_i \leftarrow \beta_m$ **end if**
4:      **if** $\pi_i = undecided$ **then**
5:          $\Delta x(t) \leftarrow \Delta x(t-1)$; $\Delta y(t) \leftarrow \Delta y(t-1)$
6:      **else**
7:          $b \leftarrow \pi_i$; $G_x \leftarrow b_x$; $G_y \leftarrow b_y$
8:          Solve $\mathcal{P}$ with respect to $\Delta x(t)$ and $\Delta y(t)$ for given G_x and G_y
9:      **end if**
10:     $\eta_i \leftarrow moving$; Give $(\Delta x(t), \Delta y(t))$ to the SFM to obtain the new position
11: **else**
12:     $\eta_i \leftarrow not\_moving$
13: **end if**

---

allocated to $x_i \in [-48, 48]$ and randomly faced either east or west. Symbols Ⓐ to Ⓨ in Fig. 1 indicate candidate positions for a visual sign employed in visual sign simulations (VSS), as discussed in Sect. 5.2.

An agent was required to choose one of two exits to evacuate the room. One was the correct exit (b^+), leading to safe evacuation, and the other (b^-) lead to an improper route, considered an evacuation failure. Thus, the agents had to select the correct exit to evacuate successfully. In our examples, the correct exits were the north and east exit for Rooms 1 and 2, respectively (both exits are indicated in blue in Fig. 1).

A visual sign κ was present (a small blue cross in Fig. 1), designating the correct exit from the room. An agent could identify the correct exit via this visual sign if it was within their visual field ($V_i \subset \{A \cup \{\kappa\}\}$). However, it was uncertain whether an agent with the correct information could always choose the correct exit, because they were also subject to herd behavior biases that could lead them to the incorrect exit. Two additional variables specified the current statuses of each agent, including a movement status $\eta_i(t) \in \{moving, not\_moving\}$, and a current decision $\pi_i(t) \in \{B \cup \{undecided\}\}$.

Using these problems, we investigated two crucial factors affecting the efficiency of crowd evacuations, including varying positions of a visual sign and varying widths of the FFV of agents. The impacts of these factors were evaluated in terms of the number of agents that chose the correct exit.

4   Agent Model

The agents in our simulations incorporated an evacuation decision model (EDM) [12,13] and a social force model (SFM) [4]. The EDM represented the herd behavior of agents during evacuations, and SFM represented physical factors affecting evacuations.

In the EDM, an agent a_i has a mental state $X_i \in \{0, 1\}$, making decisions intentionally when $X_i = 1$ and unintentionally by following the behaviors of

Algorithm 2. Agent i's action ($X_i = 1$)

1: **if** $\kappa \in V_i$ **then**
2:     $\pi_i \leftarrow b^+$
3: **else if** $\pi_i = undecided$ **then**
4:     Randomly select $b \in B$ and $\pi_i \leftarrow b$
5: **end if**
6: **if** $\pi_i = undecided$ **then**
7:     $\Delta x(t) \leftarrow \Delta x(t-1)$; $\Delta y(t) \leftarrow \Delta y(t-1)$
8: **else**
9:     $b \leftarrow \pi_i$; $G_x \leftarrow b_x$; $G_y \leftarrow b_y$
10:     Solve $\mathcal{P}$ with respect to $\Delta x(t)$ and $\Delta y(t)$ for given G_x and G_y
11: **end if**
12: $\eta_i \leftarrow moving$; Give ($\Delta x(t), \Delta y(t)$) to the SFM to obtain the new position

---

others in the agent's vicinity when $X_i = 0$. The transition probabilities between $X_i = 0$ and $X_i = 1$ are $P(X_i = 0 \rightarrow X_i = 1) = s_i^2(s_i^2 + \theta_i^2)^{-1}$ and $P(X_i = 1 \rightarrow X_i = 0) = \epsilon$, where s_i denotes a local estimation of the stimulus in the environment associated with a_i, θ_i denotes a response threshold, and ϵ denotes a constant probability common to all agents. The local estimation of stimulus in the environment is $s_i(t+1) = max\{s_i(t)+\delta-\alpha(1-R)F, 0\}$, where δ denotes an increase in the stimulus per unit time and α a scale factor of the stimulus. The variable R denotes the risk-perception function $R(r)$ of the objective risk r in the environment. We let $R(r) = (1 + e^{-g(r-\mu_i)})^{-1}$, where g denotes the activation gain affecting the shape of a sigmoid function, and μ_i denotes agent i's risk perception, representing individuals' varying sensitivities to risk. The term F denotes an evacuation progress function indicating a local observation of the total evacuation progress from the viewpoint of agent i. We let $F(n) = 1-n/N_{max}$ (if $n < N_{max}$) or 0 (otherwise), where n denotes the number of agents in a vicinity V_i and N_{max} the maximum possible number of agents in a given vicinity. The agents estimate the total progress of the evacuation using n/N_{max}, which is the population density of their vicinities.

In this simulation, we assumed the FFV of an agent as their vicinity. Thus, the range associated with the FFV of a_i (V_i) could affect (1) the estimation of the evacuation progress F, (2) agents moving in herd behavior patterns, and (3) the visual field within which an agent can recognize the visual sign κ.

Agent i executes Algorithm 1 if their mental state is $X_i = 0$ and Algorithm 2 if $X_i = 1$. Algorithm 1 represents herd behavior such that an agent selects the exit chosen by the greatest number of agents in their vicinity. Algorithm 2 represents intentional behavior pattern in which an agent chooses the designated exit if the sign is within their visual field or randomly selects an exit otherwise. A vector ($\Delta x(t), \Delta y(t)$), representing the difference between the current location and the location of an agent's next step is calculated by solving Problem $\mathcal{P}$: $min\ (x(t)+\Delta x(t)-G_x)^2+(y(t)+\Delta y(t)-G_y)^2$, subject to $\Delta x(t)^2+\Delta y(t)^2 = 1.0$.
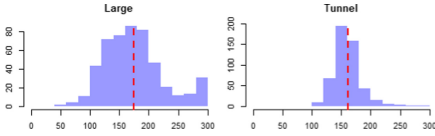
To calculate the new coordinates of an agent, we considered physical factors in the environment. Based on the desired vector ($\Delta x(t), \Delta y(t)$) (line 10 in
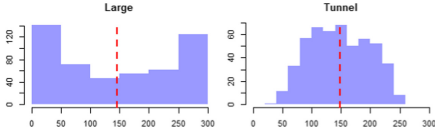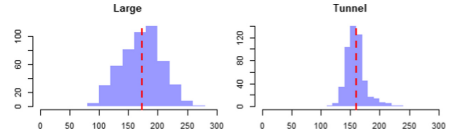
Fig. 2. Baseline histogram for Room1 (Color figure online)
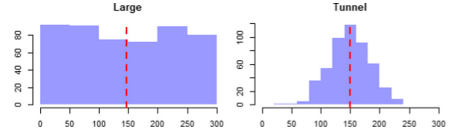
Fig. 3. Baseline histogram for Room2 (Color figure online)

Fig. 4. VSS histogram for Room1 (Color figure online)

Fig. 5. VSS histogram for Room2 (Color figure online)

Algorithm 1, and Line 12 in Algorithm 2), the SFM [4] was used to process the calculation. The parameter values used in the experiments were $\epsilon = 0.5$, $\delta = 1.0$, $\alpha = 0.5$, $N_{max} = 10$, $g = 1.0$, $d = 5$, $\Delta r = 0.5$, and $\theta_i, \mu_i \sim U(0, 100)$.

5   Experiment

We conducted experiments to explore efficient evacuation protocols through the simulation problem presented in Sect. 3. The problem aimed to maximize the number of agents selecting the correct exit (O) by varying the position of the visual sign (κ). The mean of the objective values $\bar{O}$ was adopted as the evaluation value for each sample position.

The FFV (V_i) of a_i was assumed to be a fan shape with a radius of d and an angle of ω toward each agent's heading direction. In this experiment, we investigated two types of V_i, including Large (V^L) and Tunnel (V^T). The values of d and ω for V^L and V^T were 10 120° and 10 20°, respectively.

5.1   Baseline

Prior to the experiment, we conducted baseline simulations (BS) without using a visual sign. Figure 2 depicts the histograms of 500 BSs with V^L and V^T for Room1 and Fig. 3 for Room2. The red dashed lines show the mean number of agents selecting the north exit ($\bar{O}$). Agents simply selected one of the two exits randomly in the BS; thus, the theoretical value of $\bar{O}$ was 150. Samples were distributed around $\bar{O}$; however, variances differed in each histogram. Samples far from $\bar{O}$ indicate an occurrence of exit choice pattern symmetry breaking caused by herd behaviors.

In comparison with Fig. 2 and 3, we may observe from the data shown that Room1 had larger variances than Room2. At the beginning of the simulations, all the agents flowed together in the same direction in Room1, and the flow

Large V^L

Tunnel V^T
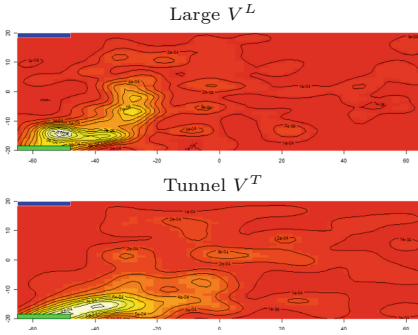
Fig. 6. Kernel density of Room1 for V^L (top) and V^T (bottom). (Color figure online)

Large V^L

Tunnel V^T
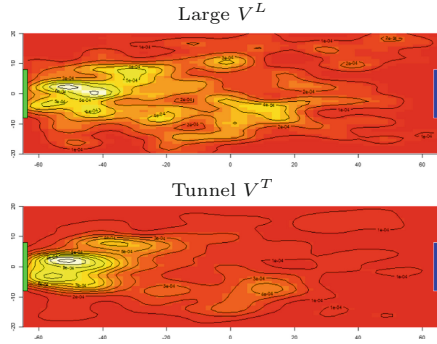
Fig. 7. Kernel density of Room2 for V^L (top) and V^T (bottom). (Color figure online)

subsequently split into two directions, whereas, in Room2, agents formed two flows in opposite directions. The results of BS are summarized in the row labeled *Base* in Table 2 in the appendix.

We also investigated the impact of evacuation information by providing information about the correct exit to a portion of the agents. In this setting, informed agents always selected the correct exit whenever $X = 1$. The ratio of informed agents and the resulting $\bar{O}$ values are summarized in Table 1 and presented in Fig. 12 and 13 for Room1 and Room2.

Table 1. Ratio of informed agents and $\bar{O}$

Ratio (%)		10	20	30	40	50	60	70	80	90
Room1	V^L	197.86	239.12	264.56	282.12	288.66	294.23	296.40	298.26	299.24
	V^T	199.56	230.16	250.91	265.69	274.70	282.75	288.27	292.56	296.35
Room2	V^L	201.32	243.30	268.41	282.33	287.20	291.58	294.38	297.04	298.62
	V^T	190.72	217.92	240.91	259.28	270.18	279.57	286.15	291.40	295.84

5.2   Visual Sign Simulation

We conducted VSS using one visual sign κ for Room1 and Room2. Five hundred positions of κ were randomly generated over $x \in [-65, 65]$ and $y \in [-25, 25]$. To estimate the value of $\bar{O}$, 10 simulations for each position were conducted.

Figure 4 shows histograms of VSS results for Room1 with V^L and V^T; the red dashed lines show the values of $\bar{O}$. Figure 5 shows the same information for Room2. Comparing the histograms from VSS and BS, we note that the presence of a single visual sign reduced variances of the results significantly. In contrast, as the mean increased in VSS, the differences were negligible, implying that the
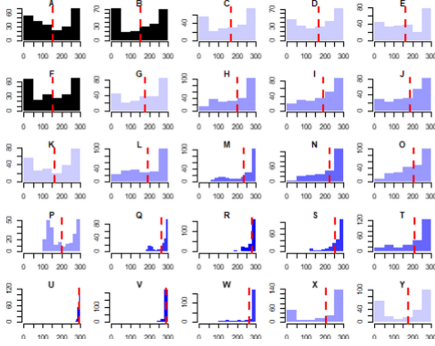
Fig. 8. Histogram of O for Ⓐ to Ⓨ for Room1 with V^L. (Color figure online)
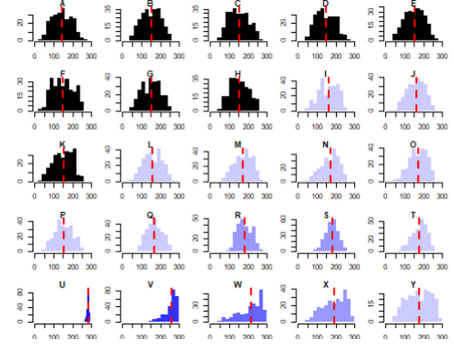
Fig. 9. Histogram of O for Ⓐ to Ⓨ for Room1 with V^T. (Color figure online)

effects were sensitive to the position of κ. The results of these simulations are summarized in the row labeled *Rand* in Table 2 in the appendix.

Figure 6 depicts heatmaps of the Kernel density of O in Room1 for V^L and V^T, from top to bottom, respectively. The Kernel density was calculated as $\hat{O} = max\{0, \ \bar{O} - 150\}$. The north exit, denoted by κ, is presented in blue, and the south exit in green. Light-colored regions represent positions of κ with high $\bar{O}$ values, indicating efficient evacuation. The same applies to Fig. 7, which belongs to Room2.

Heatmaps in Fig. 6 and 7 illustrate that the value of O changed significantly depending on location; the results were sensitive to changes in the positions of κ. If the position of κ was carefully adjusted, κ was able to guide numerous evacuees to the correct exit. However, the effect of κ could be negligible if it was improperly positioned in ineffective locations. In all the cases, the most effective position of κ was in front of the exit not designated by κ (green exits in Fig. 6 and 7). The efficient range of κ positions was not broad, especially in V^T.

We also conducted VSS with κ positions at Ⓐ to Ⓨ , as shown in in Fig. 1. Simulations were conducted 250 times for each position with V^L and V^T. Histograms of the results are presented in Fig. 8 and 9 for Room1 and in Fig. 10 and 11 for Room2; the means and standard deviations of the results are summarized in the columns labeled μ and δ in Table 2 in the Appendix. We analyzed significant differences in $\bar{O}$ between the results of VSS and BS using Welch's T-test. The P values of the t-test are also summarized in the columns labeled p in Table 2. P values with significant differences ($P < 0.05$) are indicated in italic letters in Table 2, and in blue color in Fig. 8, 9, 10 and 11. The darker the blue, the larger the mean value $\bar{O}$. Note that histograms in black show insignificant results in Fig. 8, 9, 10 and 11.

We also evaluated the results of VSS in comparison with simulations with informed agents (Table 1). Results are presented in Fig. 12 and 13 for Room1 and Room2, respectively. The x-axis shows the ratio (%) of informed agents, and the y-axis shows $\bar{O}$ values. The results with V^L are shown in blue, and
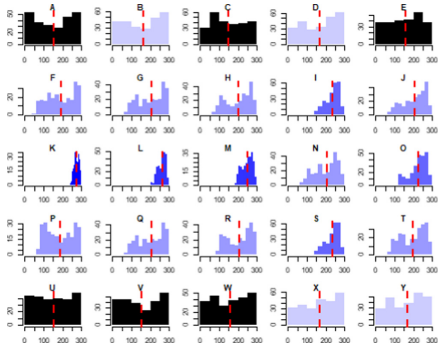
Fig. 10. Histogram of O for Ⓐ to Ⓨ for Room2 with V^L. (Color figure online)
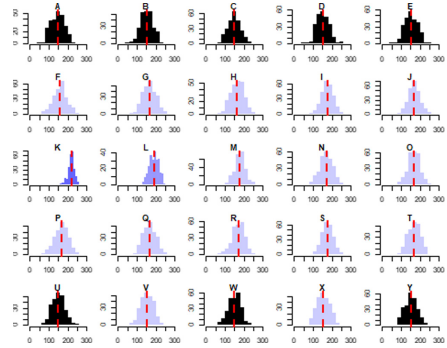
Fig. 11. Histogram of O for Ⓐ to Ⓨ for Room2 with V^T. (Color figure online)

V^T in red. Positions with $\bar{O} > 200$ in VSS are indicated on the left (V^T) and right (V^L) by corresponding letters. For example, the maximum value of $\bar{O}$ with V^L in Room1 was 293.6 (at Ⓤ), which was estimated to be equivalent to the result of conditions where 58.9 % of agents were informed (the column labeled % in Table 2). The position Ⓤ also reached a maximum $\bar{O}$ value (283.8) in the simulation with V^T, equivalent to the results with 61.8 % of agents informed. This value is almost equal to that with V^L (58.9 %). However, except for Ⓤ , these values in V^T (the column labeled % in Table 2) are significantly smaller than those in V^L. This implies that the impacts of κ were almost equivalent in V^L and V^T if the position was carefully selected. Otherwise, the effect of κ significantly dropped in V^T. The same applies to Room2; however, the values in the column labeled % were smaller than those in Room1.
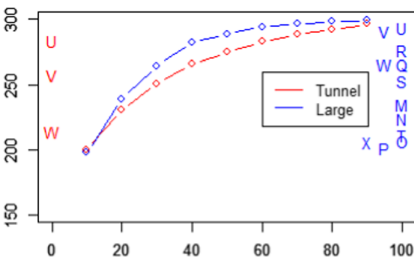
Fig. 12. $\bar{O}$ values for ratio of informed agents and κ positions for Room1. (Color figure online)
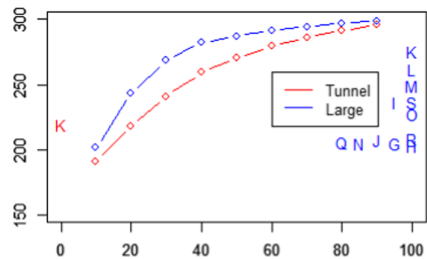
Fig. 13. $\bar{O}$ values for ratio of informed agents and κ positions for Room2. (Color figure online)

6   Discussion and Conclusion

In this study, we have assumed that excessive mental stresses or cognitive demands in evacuation situations limit human cognitive resources, leading to a narrowed visual field, which can be considered a reasonable assumption regarding tunnel vision under evacuation situations [6,7]. V^L had an area six times larger than V^T, implying significant impacts of both herd behaviors and visual sign recognition. While the broad area of V^L was efficient for visual sign recognition, it also strengthened the effects of herd behavior, decreasing the entropy in exit choice decisions (large standard deviations of V^L in Table 2), leading to an increase in incorrect exit selections. Compared with V^L, tunnel vision V^T decreased the mean number of evacuees who chose the correct exit in most positions from Ⓐ to Ⓨ ; the standard deviations also decreased in most positions. There were some cases where all evacuees chose the incorrect exit in V^L; these were rare in V^T. Because a large variance renders control difficult in general, this variance reduction in tunnel vision may easily control the evacuee behavior distribution. For example, in exploring an optimal position of visual signs through black-box optimization, large variances in V^L make estimations of mean values in each candidate point difficult, requiring many attempts in a trial-and-error method. Reduction in variances in V^T may lead to a decrease in the number of iterations required for optimization. However, this does not immediately mean that efficient positions for visual evacuation signs may be easily obtained.

VSS experiments in Room1 and Room2 showed that the results of visual sign positionings depended on both the FFV of evacuees and the exit layout in the room to be evacuated. Our experience with VSS implies that controlling the flow of evacuees is a key factor, but we expect it to be challenging in general. Assigning a visual sign at Ⓤ in Room1 produced surprisingly good results, such as 293.6 and 283.8 for V^L and V^T, respectively. This is a result of using just one visual sign; increasing these values by introducing more signs may be difficult. One factor accounting for this good result is that one of the evacuees' movement directions within the crowd flow tend to connect on this point, which could affect many other evacuees. However, this value dropped significantly with slight changes in the position of the sign, especially in the case of V^T. Moreover, some positions had insignificant effects ($p \geq 0.05$), meaning they showed no difference to the baseline. Our experiments in this study reveal the extremely high sensitivity of the tunnel vision effect to visual sign location optimization. This finding implies that tunnel vision effects may be expected to present severe difficulties and significant design challenges in terms of optimizing visual evacuation sign positions within buildings.

In this study, we concentrated on maximizing the number of agents choosing the correct exit, ignoring another crucial objective, that of minimizing evacuation time. The evacuation time in VSS, baseline, and simulations with informed agents is summarized in Table 3 The optimum positions in VSS (Ⓤ and ⓚ for Room1 and Room2) resulted in longer evacuation times because agents moved to the incorrect exit first and changed their headings to the correct exit later. This pattern of movement may be considered unnecessary and unpreferable in evacuations; however, these issues are left for future work.

Appendix

Table 2. Columns labeled μ and δ denote mean and standard deviations of $\bar{O}$. Columns labeled p denote p values of T test with BS. Columns labeled % denote the ratio of informed agents with equivalent impact to the visual sign positioning at the position corresponding to the row name.

| | Room1 | | | | | | | | Room2 | | | | | | | |
| | $Large(V^L)$ | | | | $Tunnel(V^T)$ | | | | $Large(V^L)$ | | | | $Tunnel(V^T)$ | | | |
	μ	δ	p	%	μ	δ	p	%	μ	δ	p	%	μ	δ	p	%
Base	148.0	50.4	–	–	145.3	103.4	–	–	149.6	33.5	–	–	146.5	86.2	–	–
Rand	161.1	24.1	–	–	175.1	50.2	–	–	160.0	16.8	–	–	173.0	33.6	–	–
A	152.7	102.1	0.45	0.6	143.9	50.1	0.30	0.0	152.5	91.6	0.52	0.5	146.3	35.1	0.36	0.0
B	154.8	106.7	0.31	1.0	152.5	49.7	0.18	0.5	161.0	90.0	0.04	2.2	153.1	32.4	0.07	0.8
C	166.3	99.7	0.00	3.4	151.3	51.3	0.33	0.3	149.8	84.0	0.83	0.0	149.2	33.4	0.86	0.0
D	167.6	98.6	0.00	3.7	146.9	49.5	0.84	0.0	168.1	87.3	0.00	3.5	152.1	32.5	0.16	0.5
E	164.7	98.3	0.01	3.1	154.0	51.2	0.08	0.8	156.3	81.9	0.15	1.2	153.4	33.8	0.06	0.8
F	154.3	102.3	0.32	0.9	149.2	53.7	0.69	0.0	192.8	71.9	0.00	8.3	160.5	36.0	0.00	2.6
G	177.8	95.7	0.00	5.8	151.9	48.2	0.23	0.4	205.1	66.6	0.00	10.9	167.1	34.1	0.00	4.2
H	199.4	85.6	0.00	10.4	154.5	49.2	0.05	0.9	202.7	65.6	0.00	10.3	165.2	34.7	0.00	3.7
I	194.0	84.4	0.00	9.2	160.9	48.4	0.00	2.2	236.6	35.5	0.00	18.4	176.8	29.6	0.00	6.6
J	187.8	88.8	0.00	7.9	160.6	47.1	0.00	2.2	207.0	60.4	0.00	11.4	169.9	29.6	0.00	4.9
K	164.5	100.6	0.01	3.0	151.8	50.5	0.25	0.4	275.7	13.6	0.00	35.3	219.4	16.9	0.00	20.6
L	193.0	91.7	0.00	9.0	160.6	48.4	0.00	2.1	262.0	21.3	0.00	27.5	191.6	24.0	0.00	10.3
M	234.6	70.2	0.00	18.9	174.3	46.3	0.00	4.9	248.8	28.6	0.00	22.2	179.6	27.4	0.00	7.3
N	223.5	72.7	0.00	16.2	170.5	46.5	0.00	4.1	204.3	60.1	0.00	10.7	170.5	32.4	0.00	5.1
O	206.3	75.2	0.00	12.1	172.1	45.8	0.00	4.5	205.1	43.6	0.00	16.2	167.9	30.4	0.00	4.4
P	201.2	68.1	0.00	10.8	154.6	47.1	0.04	0.9	186.1	70.6	0.00	7.0	167.3	35.7	0.00	4.3
Q	265.0	37.8	0.00	30.2	170.2	41.3	0.00	4.1	205.1	66.6	0.00	10.9	167.1	34.1	0.00	4.2
R	276.5	29.2	0.00	36.8	182.4	39.9	0.00	6.5	208.1	62.7	0.00	11.6	171.0	33.8	0.00	5.2
S	252.4	52.4	0.00	25.2	180.0	34.6	0.00	6.1	236.6	35.5	0.00	18.4	176.8	29.6	0.00	6.6
T	211.4	84.9	0.00	13.3	178.8	40.7	0.00	5.8	198.6	63.7	0.00	9.5	169.3	32.6	0.00	4.7
U	293.6	5.2	0.00	58.9	283.8	6.1	0.00	61.8	151.4	88.3	0.64	0.3	150.7	33.7	0.43	0.2
V	290.6	17.3	0.00	53.5	257.2	32.5	0.00	34.2	154.8	89.7	0.29	0.9	153.8	33.7	0.05	0.9
W	265.7	55.1	0.00	30.6	214.2	61.2	0.00	14.8	156.9	87.5	0.15	1.3	150.8	33.0	0.39	0.2
X	205.6	106.5	0.00	11.9	192.4	60.3	0.00	8.6	166.5	86.0	0.00	3.2	154.5	33.1	0.02	1.1
Y	176.0	112.9	0.00	5.4	175.5	63.2	0.00	5.1	166.6	83.2	0.00	3.2	152.1	32.5	0.17	0.5

Table 3. Evacuation time of VSS (Ⓤ and Ⓚ for Room1 and Room2), baseline, and 100% informed agent simulation. Means and standard deviations are provided in the columns labeled μ and δ.

| | (V^T) | | | | | | (V^L) | | | | | |
| | VSS | | Baseline | | 100% | | VSS | | Baseline | | 100% | |
	μ	δ	μ	δ	μ	δ	μ	δ	μ	δ	μ	δ
Room1	193.14	10.48	168.93	9.88	170.56	10.20	148.73	8.68	143.27	4.88	146.13	3.29
Room2	232.80	19.95	169.23	12.49	176.10	8.21	196.94	32.91	147.14	19.04	167.91	9.80

References

1. Burke, A., Heuer, F., Reisberg, D.: Remembering emotional events. Memory Cogn. **20**, 277–290 (1992)
2. Christianson, S.A.: Emotional stress and eyewitness memory: a critical review. Psyhol. Bull. **112**(2), 284–309 (1992)
3. Christianson, S.A., Loftus, E.F.: Memory for traumatic events. Appl. Cogn. Psychol. **1**(4), 225–239 (1987)
4. Helbing, D., Farkas, I., Vicsek, T.: Simulating dynamical features of escape panic. Nature **407**(28), 487–490 (2000)
5. Li, X., Guo, F., Kuang, H., Geng, Z., Fan, Y.: An extended cost potential field cellular automaton model for pedestrian evacuation considering the restriction of visual field. Physica A Stat. Mech. Appl. **515**, 47–56 (2019)
6. Loftus, E., Loftus, G., Messo, J.: Some facts about "weapon focus". Law Hum. Behav. **11**, 55 (1987)
7. Mackworth, N.H.: Visual noise causes tunnel vision. Psychon. Sci. 67–68 (1965). https://doi.org/10.3758/BF03343023
8. Mas, E., Suppasri, A., Imamura, F., Koshimura, S.: Agent-based simulation of the 2011 great East Japan earthquake/tsunami evacuation: an integrated model of tsunami inundation and evacuation. J. Nat. Dis. Sci. **34**(1), 41–57 (2012)
9. Meng, F., Zhang, W.: Way-finding during a fire emergency: an experimental study in a virtual environment. Ergonomics **57**, 816–827 (2014)
10. Moussad, M., Schinazi, V.R., Kapadia, M., Thrash, T.: Virtual sensing and virtual reality: how new technologies can boost research on crowd dynamics. Front. Robot. AI **5**, 1–14 (2018)
11. Moussaïd, M., Helbing, D., Theraulaz, G.: How simple rules determine pedestrian behavior and crowd disasters. Proc. Natl. Acad. Sci. **108**(17), 6884–6888 (2011)
12. Tsurushima, A.: Modeling herd behavior caused by evacuation decision making using response threshold. In: Davidsson, P., Verhagen, H. (eds.) MABS 2018. LNCS (LNAI), vol. 11463, pp. 138–152. Springer, Cham (2019). https://doi.org/10.1007/978-3-030-22270-3_11
13. Tsurushima, A.: Symmetry breaking in evacuation exit choice: impacts of cognitive bias and physical factor on evacuation decision. In: van den Herik, J., Rocha, A.P., Steels, L. (eds.) ICAART 2019. LNCS (LNAI), vol. 11978, pp. 293–316. Springer, Cham (2019). https://doi.org/10.1007/978-3-030-37494-5_15
14. Tsurushima., A.: Reproducing evacuation behaviors of evacuees during the great East Japan earthquake using the evacuation decision model with realistic settings. In: Proceedings of the 13th International Conference on Agents and Artificial Intelligence - Volume 1: ICAART, pp. 17–27. INSTICC, SciTePress (2021). https://doi.org/10.5220/0010167700170027
15. Tucker, A., March, K.L., Gifford, T.: The effects of information and hazard on evacuee behavior in virtual reality. Fire Saf. J. **99**, 1–11 (2018)
16. Wijerathne, M., Melgar, L., Hori, M., Ichimura, T., Tanaka, S.: HPC enhanced large urban area evacuation simulations with vision based autonomously navigating multi agents. Procedia Comput. Sci. **18**, 1515–1524 (2013). 2013 International Conference on Computational Science

17. Xu, Y., Huang, H.J.: Simulation of exit choosing in pedestrian evacuation with consideration of the direction visual field. Physica A Stat. Mech. Appl. **391**(4), 991–1000 (2012)
18. Yue, H., Guan, H., Shao, C., Liu, Y.: Simulation of pedestrian evacuation with affected visual field and absence of evacuation signs. In: 2010 Sixth International Conference on Natural Computation, vol. 8, pp. 4286–4290 (2010)